Serial Assessment of Human Tumor Burdens in Mice by the Analysis of Circulating DNA

Carlo Rago,[1,2] David L. Huso,[2,3] Frank Diehl,[1,2] Baktiar Karim,[3] Guosheng Liu,[3] Nickolas Papadopoulos,[1,2] Yardena Samuels,[1] Victor E. Velculescu,[1] Bert Vogelstein,[1,2] Kenneth W. Kinzler,[1,2] and Luis A. Diaz, Jr.[1,2]

[1]The Ludwig Center for Cancer Genetics and Therapeutics and The Howard Hughes Medical Institute, [2]The Sidney Kimmel Comprehensive Cancer Center, and [3]Department of Molecular and Comparative Pathobiology, The Johns Hopkins Medical Institutions, Baltimore, Maryland

Abstract

Internal human xenografts provide valuable animal models to study the microenvironments and metastatic processes occurring in human cancers. However, the use of such models is hampered by the logistical difficulties of reproducibly and simply assessing tumor burden. We developed a high-sensitivity assay for quantifying human DNA in small volumes of mouse plasma, enabling in-life monitoring of systemic tumor burden. Growth kinetics analyses of various xenograft models showed the utility of circulating human DNA as a biomarker. We found that human DNA concentration reproducibly increased with disease progression and decreased after successful therapeutic intervention. A marked, transient spike in circulating human tumor DNA occurred immediately after cytotoxic therapy or surgery. This simple assay may find broad utility in target validation studies and preclinical drug development programs. [Cancer Res 2007;67(19):9364–70]

Introduction

Animal models have been essential to our understanding of human cancer. Subcutaneous tumors in mice are most often used to evaluate issues relating to tumorigenicity and therapy, as tumor growth can be easily measured in such systems by visual inspection. However, it is increasingly recognized that host stroma plays a major role in tumorigenesis and that the stromal factors in internal organs such as liver and lung are not the same as those in subcutaneous tissues (1–5). Cancer researchers are therefore gradually turning to human xenograft models in which tumors are formed internally, either through metastasis or implantation, to more accurately mimic human disease (6, 7).

The major experimental problem with internal tumors is their quantitative assessment. Accordingly, many sophisticated methods have been devised to follow such tumors in mice. Direct imaging methods, such as magnetic resonance imaging or computed tomography, are useful in this regard but they can only detect relatively large tumors and require expensive equipment (8). Imaging with fluorescent or luminescent markers provides much greater sensitivity but also requires genetic engineering of the cell lines to introduce markers (9). The introduction of such markers can itself alter the growth characteristics of tumors (10). Moreover, direct or indirect imaging methods require that animals be anaesthetized and the imaging process takes a considerable amount of time. Imaging methods are therefore not well-suited for situations in which multiple sequential measurements on many mice are desirable.

In light of these problems, several studies have evaluated biochemical measurements *ex vivo* for internal tumor assessment. For example, tumor cells engineered to secrete human chorionic gonadotrophin can be monitored through the evaluation of the urine (11). Like the imaging methods noted above, this approach requires genetic engineering of each cell line to be evaluated. A more generally applicable approach is to use human DNA as a marker of tumor burden. Indeed, the concentration of human DNA sequences can be quantitatively assessed by real-time PCR and this principle has been applied to measure human tumor cells in the solid organs of mice, rats, and chickens (12–15). There has also been one recent report of the application of this approach to circulating DNA in mice harboring human ovarian xenografts (16). However, the DNA quantification method described in ref. 16 required the sacrifice of the mice to collect sufficient plasma for detection of human sequences. We have independently developed a facile approach that is more sensitive and allows repeated measurements from small amounts of plasma (<25 μL) collected from the tail veins of mice. As shown below, this technique can be effectively used to monitor the development of tumors in a variety of models and to track the efficacy of therapeutic measures.

Materials and Methods

Animals, cell lines, and reagents. All experimental procedures were in compliance with U.S. laws governing animal experimentation and were approved and overseen by the Johns Hopkins University Animal Care and Use Committee. Female athymic nude mice 3 to 8 weeks of age were purchased from Harlan. The HCT116 parental cell line and a derivative clone retaining only the mutant *PIK3CA* allele were derived as previously described (17). The thymidine kinase expressing osteosarcoma (143B-PML-BK-TK) and the LS 174T colorectal adenocarcinoma (ATCC no. CL-188) cell lines were obtained from American Type Culture Collection. All cell lines were grown as monolayers in McCoy's 5A medium (Invitrogen) supplemented with 10% fetal bovine serum (HyClone) and 0.9% penicillin-streptomycin solution (Invitrogen) at 37°C and 5% CO_2. Ganciclovir was purchased from Roche and used at 100 mg/kg delivered by i.p. injection.

Subcutaneous and metastatic tumor models. Suspensions of 5×10^6 HCT116 parental cells in 0.1 mL of culture media were injected s.c. into the flank of mice. Tumors were measured with an electronic digital caliper (AVID) at the time indicated in the text. Tumor volume was calculated as length (L) × width^2 (W) × 0.5. Metastatic models were established by injection of one million tumor cells in 500 μL of 1× PBS (HCT116) or 100 μL of McCoy's 5A medium (Cl-188) via the tail vein.

Orthotopic and ectopic tumor models. Tumor fragments were prepared via s.c. injection of 1×10^5 HCT116 or 143B cells in the flank of athymic nude mice. After subcutaneous tumors reached a size of 500 to 1,000 mm^3, the mice were euthanized and the tumors were removed and

Requests for reprints: Luis A. Diaz, Johns Hopkins Kimmel Comprehensive Cancer Center, 1650 Orleans Street, Cancer Research Building I, Room 590, Baltimore, MD 21231. Phone: 410-955-8878; Fax: 410-955-0548; E-mail: ldiaz1@jhmi.edu.

doi:10.1158/0008-5472.CAN-07-0605

placed in ice-cold 1× PBS (Invitrogen). For internal tumor implantation, athymic nude female mice were anesthetized with isoflurane (SurgiVet) and the abdomen was scrubbed for surgery. A small incision was made parallel to the linea alba and the cecum was exteriorized. A single fragment of tumor of ~1 mm^3 in size was implanted on the serosal surface. An absorbable suture (3–0 Vicryl) was used to attach the tumor to the serosal wall without penetrating the inner layers of the intestine. The organ was returned to the abdominal cavity, and the abdominal wall was closed. For transplantation to hepatic sites, an incision was made in the ventral left upper abdominal quadrant. The left lobe of the liver was carefully exposed and a blunt needle was used to puncture the liver capsule. A single fragment of tumor of ~0.5 mm^3 in size was then placed in the hole made by the needle. After hemostasis, the abdomen and skin were closed.

Plasma preparation. Whole venous blood was accessed by tail prick with a 26 1/2–gauge needle or scalpel blade and collected directly into a disposable EDTA-coated plastic capillary tube (Hematronics) or aspirated by pipette. Twenty-five microliters of whole blood was added to 200 μL of 1× PBS containing 4.5 mmol/L of EDTA (Invitrogen) in a 1.5 mL polypropylene tube (Corning Life Sciences) and subjected to centrifugation at 1,500 × *g* for 15 min at room temperature. Plasma was aliquoted and frozen at −80°C.

Human *LINE* quantification. DNA was purified from 100 μL of the diluted plasma samples using the QIAamp DNA micro kit (Qiagen) as recommended by the manufacturer with 1 μL of carrier RNA per 100 μL of AL buffer, eluted in 40 μL of EB buffer, and stored at −80°C. PCR was done in 25 μL with the following components: 13.75 μL sterile tissue culture grade double-distilled water (Invitrogen), 2.5 μL of 10× PCR buffer, 2.5 μL of 10 mmol/L deoxynucleotide triphosphates (U.S. Biochemical) 1.5 μL of DMSO (Sigma), 0.5 μL of SYBR Green I solution (Invitrogen) diluted 1:1,000 in double-distilled water, 0.5 μL of 50 μmol/L forward primer FWD 5′-TCACTCAAAGCCGCTCAACTAC-3′ (Invitrogen; desalted, 25 nmol scale), 0.5 μL of 50 μmol/L reverse primer REV 5′-TCTGCCTTCATTTCGTTATG-TACC-3′ (Invitrogen; desalted, 25 nmol scale), 0.25 μL of Platinum taq DNA polymerase (Invitrogen), and 3 μL of purified DNA. The 10× PCR buffer contained 670 mmol/L of Tris-HCl (pH 8.8), 67 mmol/L of $MgCl_2$, 166 mmol/L of $(NH_4)_2SO_4$, and 100 mmol/L of 2-mercaptoethanol (18). Purified DNA from plasma was used directly without further dilution. The reaction was monitored on an iCycler (Bio-Rad) with the following cycling conditions: (94°C, 2 min) × 1, (94°C, 10 s; 67°C, 15 s; 70°C, 15 s) × 3, (94°C, 10 s; 64°C, 15 s; 70°C, 15 s) × 3, (94°C, 10 s; 61°C, 15 s; 70°C, 15 s) × 3, (94°C, 10 s; 59°C, 15 s; 70°C, 15 s) × 35. The threshold cycle number was determined using Bio-Rad analysis software (version 3.0.6070) with the PCR baseline subtracted. Various dilutions of normal human DNA purified from lymphocytes were incorporated in each plate to serve as standards. The numbers of mice per group are noted in the figure legends and all experiments were repeated at least twice with similar results.

Statistical analysis. Data are presented as mean ± SD. Student's *t* test (unpaired) was used as indicated in the text to compare continuous variables. The statistical significance level was set at $P < 0.05$.

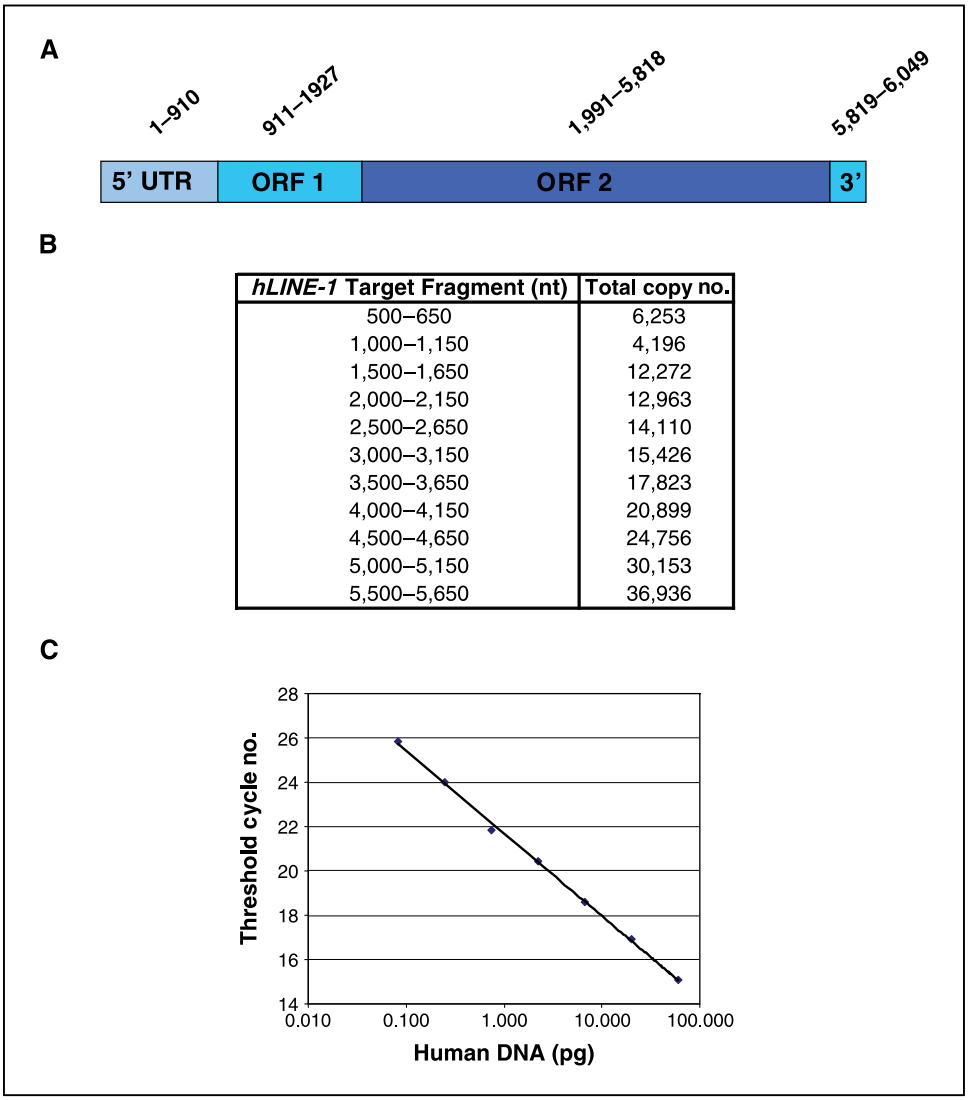

hLINE-1 Target Fragment (nt)	Total copy no.
500–650	6,253
1,000–1,150	4,196
1,500–1,650	12,272
2,000–2,150	12,963
2,500–2,650	14,110
3,000–3,150	15,426
3,500–3,650	17,823
4,000–4,150	20,899
4,500–4,650	24,756
5,000–5,150	30,153
5,500–5,650	36,936

Figure 1. Human LINE-1 sequences and assay development. *A,* the *hLINE-1* structure with nucleotide positions depicted. *B,* 81,587 *hLINE-1* entries were retrieved from GenBank using accession no. M80343. Sequence positions of the canonical *hLINE-1* were used to search these 81,587 family members and determine their copy number. This copy number map defined regions of high abundance and helped focus primer design. The optimized primer set spans nucleotide positions 2715 to 2796. *C,* correlation between threshold cycles and amount of human DNA added to a PCR reaction in a typical PLOT assay. Essentially identical results were obtained in >10 replicates of this experiment, with threshold cycles varying by <0.3 at any DNA concentration used.

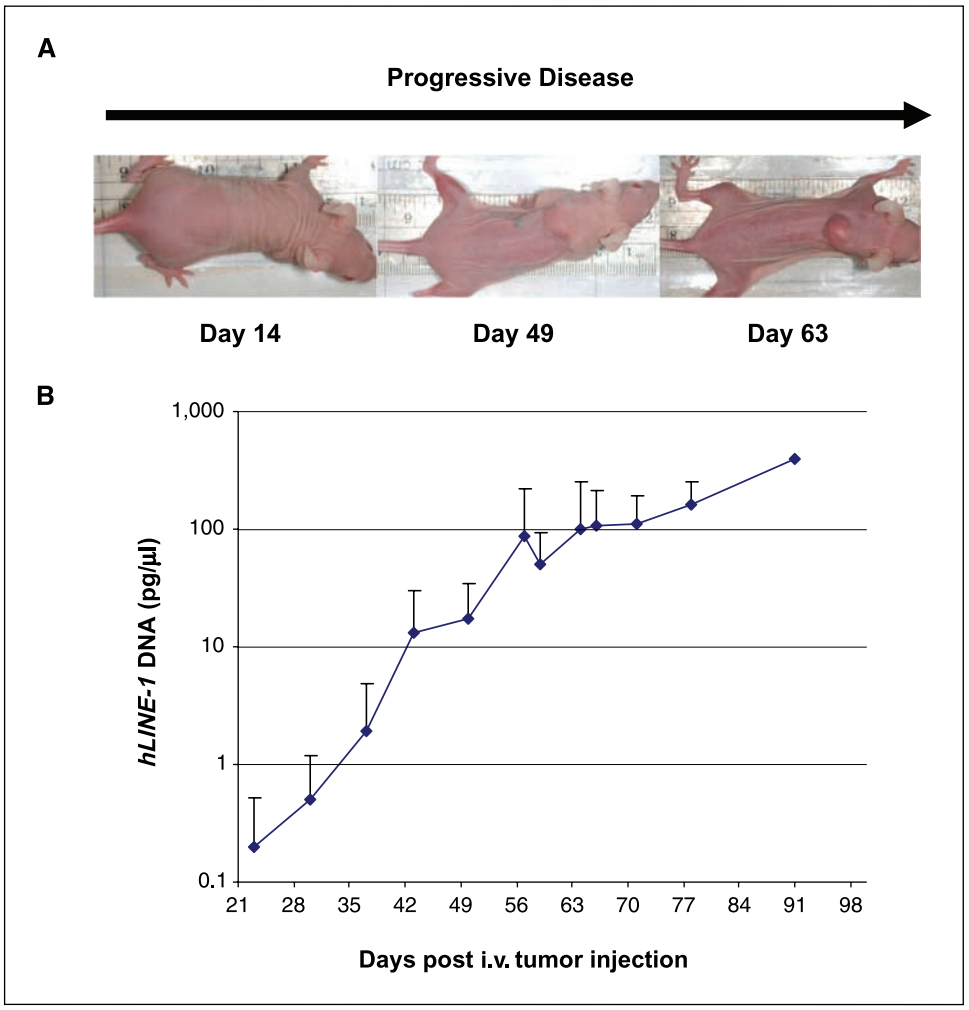

Figure 2. Circulating *hLINE-1* DNA following i.v. injection of tumor cells. *A,* images of the typical course of human cancer progression in athymic nude mice following i.v. injection of HCT116 cells with metastatic potential. *B,* mean plasma *hLINE-1* DNA concentrations from 10 mice evaluated at the indicated times after i.v. injection of tumor cells. *Points,* means; *bars,* SD.

Results

High-sensitivity detection of human DNA in mouse plasma. To measure systemic xenograft burdens in various mouse models, we sought to develop a sensitive method for quantifying human DNA in small volumes of mouse plasma. The human long interspersed nuclear element-1 (*hLINE-1*) retrotransposon family members were ideal for this purpose because ~100,000 of these elements exist in the human genome and, as shown below, a subset of these copies can be distinguished from mouse orthologues (19). The prototypical human LINE-1 consists of a 5′ untranslated region (5′-UTR; nucleotide, 1–910), open reading frame (ORF) 1 (nucleotide, 911–1927), ORF2 (nucleotide, 1991–5818), and a 3′-UTR (nucleotide, 5819–6049) as depicted in Fig. 1*A*. Using the BLAST algorithm (20), we found 81,587 matches of the canonical *hLINE-1* (GenBank accession no. M80343) sequence in the human genome. Because members of the *hLINE-1* family are known to be truncated (21), we generated a copy number map that allowed us to exclude regions with low abundance from primer design (Fig. 1*B*). The nucleotide start and stop positions for each entry were used to determine the presence of *hLINE-1* subfragments among family members. For example, we found that the 5′-UTR was frequently truncated such that nucleotide positions 500 to 650 were only found in 6,253 (7.7%) of the 81,587 matches. On the other hand, the 3′-end of ORF2 (nucleotide positions, 5500–5650) was found within 36,936 *hLINE-1* elements, representing 45.3% of all entries. Because *hLINE-1* family members are divergent at the nucleotide level, we used the BLAT algorithm (22) to confirm the number of exact matches in the human genome for each candidate primer (data not shown) before they were tested empirically.

Optimization of human *LINE-1* primer specificity. In silico PCR (23) was used to eliminate candidate primer sets that were predicted to amplify mouse DNA, as sequences related to *hLINE-1* are present in mice. The high sequence similarity of the mouse *Igl* gene (GenBank accession no. NG_004051) made this gene particularly difficult to exclude. As we expected that human DNA would represent only a tiny fraction of the total DNA present in the plasma of mice with tumors, it was critical to avoid any amplification of mouse DNA. We therefore focused on regions of *hLINE-1* that were highly represented in the human genome but which were as unrelated as possible to those in mouse. Empirical testing of >30 primer combinations using human and mouse DNA templates eventually allowed us to identify a primer set (see Materials and Methods) that amplified abundant human sequences within ORF2 but did not coamplify mouse sequences. The amplicon generated from the optimal primer set contained nucleotide positions 2715 to 2796. Control experiments showed that there was a linear correlation between the amount of human DNA and the log of the threshold cycle number of real-time PCR data (Fig. 1*C*).

The resultant assay was termed plasma *LINE-1* optimized threshold (PLOT). Mouse plasma did not inhibit this assay when

done as described in Materials and Methods, and the limit of detection was ~0.06 pg of human DNA/μL plasma or ~0.01 human cell genomes/μL of plasma. This limit was defined by PCR signals that arise at ~25 to 27 cycles in plasma from mice without tumors, presumably due to background human DNA contamination. These background levels were consistent with the effective laboratory background of human DNA as defined by forensic criteria to be 0.0174 pg/μL with a range between 0.0119 and 0.0549 pg/μL (24).

Biological and technical issues. Studies in humans have shown that tumor DNA is often present in the plasma of cancer patients, particularly those with metastatic disease (25, 26). In such patients, the tumor DNA is generally degraded and amplicons of small size (~100 bases) are required for detection (27). We assumed that the plasma DNA from human xenografts would similarly be degraded. The primer set used for PLOT generated an 82 bp amplicon, allowing the detection of small circulating *hLINE-1* DNA molecules. In the metastatic models described below, we found that this 82 bp *hLINE-1* DNA fragment was ~8- to 10-fold more highly represented in mouse plasma than a 150 bp fragment encompassing it, presumably due to degradation of the larger fragments in plasma. It is important to note that fragments of *hLINE-1* are ubiquitous wherever humans are found. In the course of method development, we found that the maximum sensitivity of the assay was affected by the scale and source of primers. We compared primers from various commercial suppliers and found that the desalted, 25 nmol scale synthesis from Invitrogen yielded the least amount of contamination. In addition, every new batch of primer, as well as every component of the PCR mix, was carefully screened to ensure that it was not contaminated with human DNA.

PLOT in experimental models of malignancy. To determine whether *hLINE-1* sequences could be detected in the plasma of mice bearing human tumor xenografts, we injected human colorectal cancer cells into the tail vein of athymic nude mice. The cell line chosen was an HCT116 derivative in which the wild-type *PIK3CA* allele was inactivated by targeted homologous integration. This cell line retained an endogenous mutant *PIK3CA* allele (arginine substituted for histidine at codon 1047) and metastasized widely when systemically injected into nude mice (17). The mice developed cachexia and metastatic deposits in a variety of target organs over 8 to 16 weeks (Fig. 2*A*). Ten mice were injected with tumor cells and serial blood samples of 25 μL were taken from the tail vein. From these samples, the plasma fraction was collected, DNA was purified and the hLINE-1 content was measured by quantitative PCR (Fig. 2*B*). In tumor-bearing mice, *hLINE-1* DNA became detectable in plasma 23 days after i.v. injection of cells. This was weeks before any animal developed tumors (Fig. 2*A*) or developed any other signs of illness. The quantity of *hLINE-1* DNA increased with time and plateaued at ~60 days following injection. The assay also provided a large dynamic range, apparent in Fig. 2*B*, with plasma *hLINE-1* DNA increasing by >1,000-fold over the course of the experiment.

To determine if plasma DNA could be used to monitor tumor progression in other tumor models, three additional systems were studied. Two systems employed HCT116 tumor fragments which were implanted orthotopically onto the cecum (Fig. 3*A*) or directly into the liver (Fig. 3*B*). A third system involved the i.v. injection of a colorectal cancer line, CL-188 (Fig. 3*C*; ref. 28). In all three of these models, *hLINE-1* DNA became detectable in the plasma within 8 to 17 days following tumor initiation. As with the experiment depicted in Fig. 2, the concentrations of plasma *hLINE-1* DNA were very similar in mice sampled at identical time

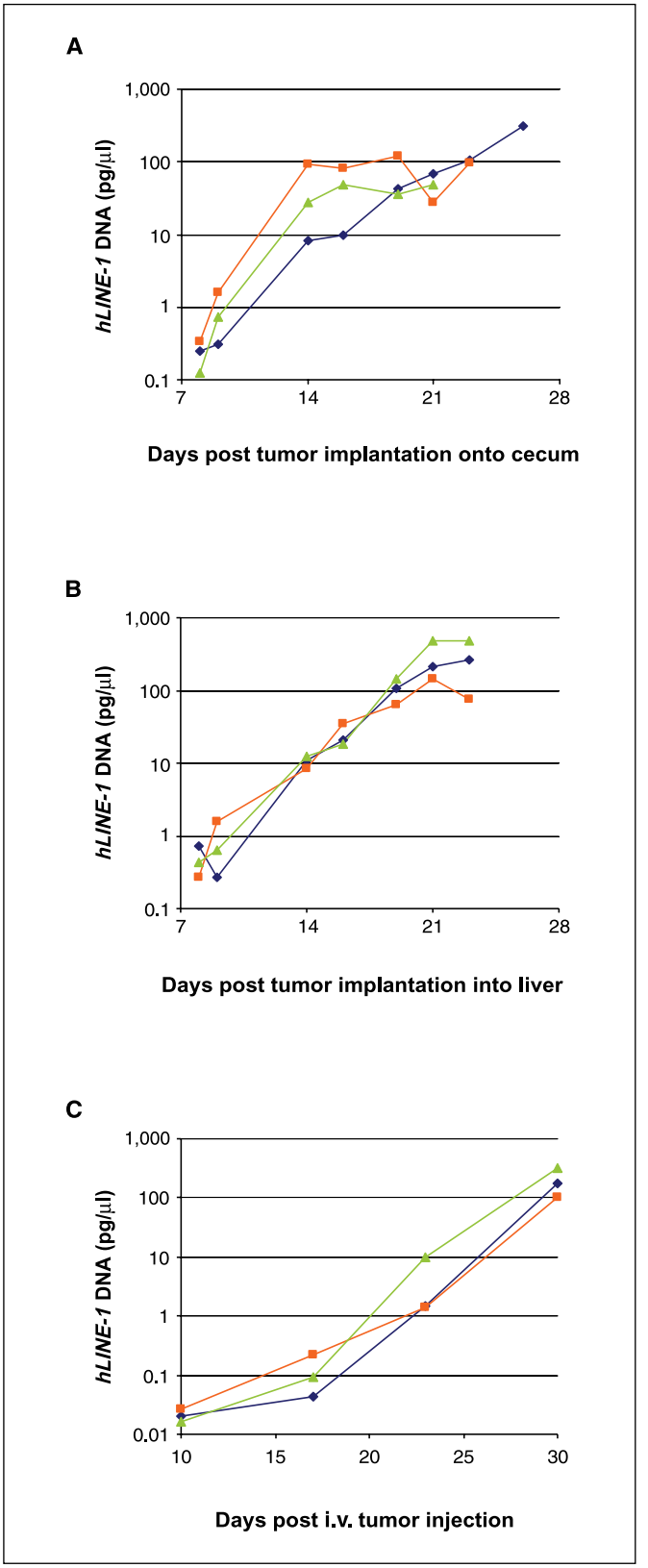

Figure 3. Circulating *hLINE-1* DNA in various tumor models. The concentration of plasma *hLINE-1* DNA in individual athymic nude mice was determined at the indicated times after orthotopic transplantation of HCT116 tumor fragments to the cecum (*A*), direct transplantation of HCT116 tumor fragments to the liver (*B*), or i.v. injection of CL-188 colorectal adenocarcinoma cells (*C*). Three mice for each model are represented individually in *A–C*.

points. The data in Fig. 3 also illustrates that individual mice can be readily followed over time and that internal tumor progression in each mouse can be readily monitored in a noninvasive manner.

Concentration of plasma *hLINE-1* DNA is related to tumor volume. To determine the relationship between tumor burden and plasma *hLINE-1* DNA, we established subcutaneous tumors from HCT116 cells. Tumors became evident 5 to 7 days after injection and increased in size by ~5.5-fold between days 11 and 25, with growth slowing thereafter (Fig. 4*A*). Plasma *hLINE-1* DNA became detectable 10 days after injection, increased ~5.8-fold between days 11 and 25, then plateaued (Fig. 4*B*). Note that tumor volume is only an approximate measure of viable tumor cells, as tumors contain necrotic regions, particularly as they reach large sizes, as well as nonneoplastic cells. Likewise, circulating DNA is only an approximate measure of tumor burden as it reflects dynamic states involving necrosis and apoptosis (29). Given these uncertainties, the data in Fig. 4 show a reasonable correlation between plasma *hLINE-1* DNA and tumor bulk. Interestingly, plasma *hLINE-1* DNA concentrations were considerably lower in mice with subcutaneous tumors compared with internal tumors (compare Fig. 4 with Figs. 2 and 3, noting the different scales for the *Y*-axis). This could be a result of the lack of invasiveness of subcutaneous compared with internal tumors. Alternatively, subcutaneous tumors may have fewer neoplastic cells per cross-sectional tumor burden than internal tumors, leading to less circulating tumor-specific DNA.

The subcutaneous tumor model also provided a means to determine the half-life of *hLINE-1* DNA in plasma. Tumors were surgically removed at day 40, resulting in an 86% decrease in plasma *hLINE-1* DNA 6 h later (Fig. 4*B*). By 29 h, plasma *hLINE-1* DNA was no longer detectable over the background levels.

PLOT as a biomarker for therapeutic response. The correlation between plasma *hLINE-1* DNA and tumor burden and its rapid decline after tumor excision suggested that plasma *hLINE-1* DNA might serve as a biomarker for nonsurgical forms of therapy. To test this possibility, we used an osteosarcoma cell line (OSTK) that had been modified to express thymidine kinase, thereby making it highly sensitive to ganciclovir. Tumor fragments from a subcutaneous xenograft of OSTK were implanted in the livers of athymic nude mice. The mice were then treated daily with ganciclovir or with vehicle alone on days 20 to 24. A potent therapeutic response was observed as *hLINE-1* DNA levels in the treated group showed an initial increase followed by a decrease to below pretreatment levels by day 27. This pattern was not observed in the control group (Fig. 5*A*). A linear plot from individual mice revealed a cumulative treatment-related spike in *hLINE-1* DNA at day 23. This was present in all mice evaluated (one representative example is shown in Fig. 5*B*). On average, a 7.5-fold spike in plasma *hLINE-1* DNA was noted in ganciclovir-treated mice, in contrast to mice treated with vehicle alone ($P < 0.05$, unpaired t test) where no such spike was observed. Dissection of mice following therapy confirmed the eradication of tumor in all treated mice and the persistence of tumor in control mice, with an average tumor volume of 3.19 ± 1.75 cm^3 SD at necropsy.

To compare the results of chemotherapy in this model with those of surgery, we surgically resected the lobe of the liver into which tumor fragments had been injected 27 days earlier. Prior to surgical resection, serial measurements showed gradually increasing plasma *hLINE-1* DNA concentrations. Immediately after tumor resection, all mice exhibited a spike in *hLINE-1* DNA levels (Fig. 5*C*). Within a few hours thereafter, a rapid decline in plasma *hLINE-1* DNA levels was noted in all mice.

Discussion

These results show that circulating DNA can be used to monitor neoplastic development in mice bearing human xenograft tumors in a variety of organs. Additionally, they show that plasma *hLINE-1* DNA is an excellent indicator of the response to therapy. In this regard, a decrease in plasma *hLINE-1* DNA routinely occurred after treatment with chemotherapy or surgery. What was more surprising was the seemingly paradoxical increase in plasma *hLINE-1* DNA that occurred immediately following chemotherapeutic treatment or surgery and before a decrease became apparent. Evidently, cytotoxic agents cause the release of a burst of tumor DNA into the circulation. Similarly, the tumor resection itself may have caused tumor cell death resulting in a release of tumor DNA into the circulation during the surgical procedure. Transient increases in tumor DNA in the circulation following therapy are not unprecedented. In humans, circulating EBV DNA seem to increase after surgical resection of nasopharyngeal carcinomas (30). While the current study was in progress, Kamat et al. reported that circulating tumor DNA increased 1 day following treatment of intraperitoneal ovarian tumors with docetaxel (16).

In aggregate, these studies suggest that the assay of circulating tumor-specific DNA will be generally useful for the study of human xenografts in cancer biology and drug discovery. The observations

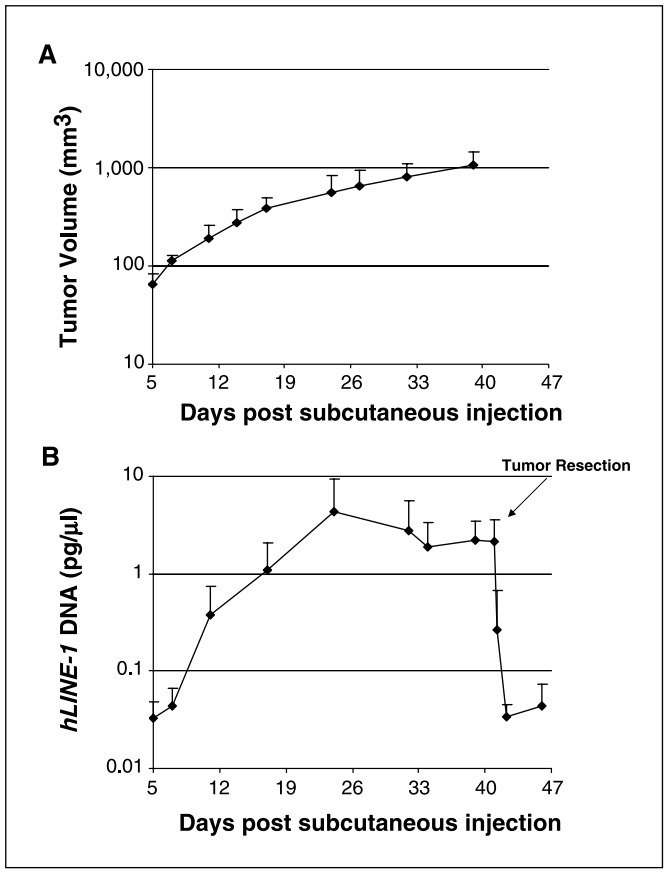

Figure 4. Circulating *hLINE-1* DNA levels correlate with tumor burden. *A,* tumor volumes were measured in athymic nude mice bearing subcutaneous HCT116 human colon cancer cells ($n = 4$). *B,* the tumors were surgically excised 41 d (*arrow*) after implantation. Plasma was serially acquired from these mice and *hLINE-1* concentrations were measured at the indicated times. *Points,* means; *bars,* SD.

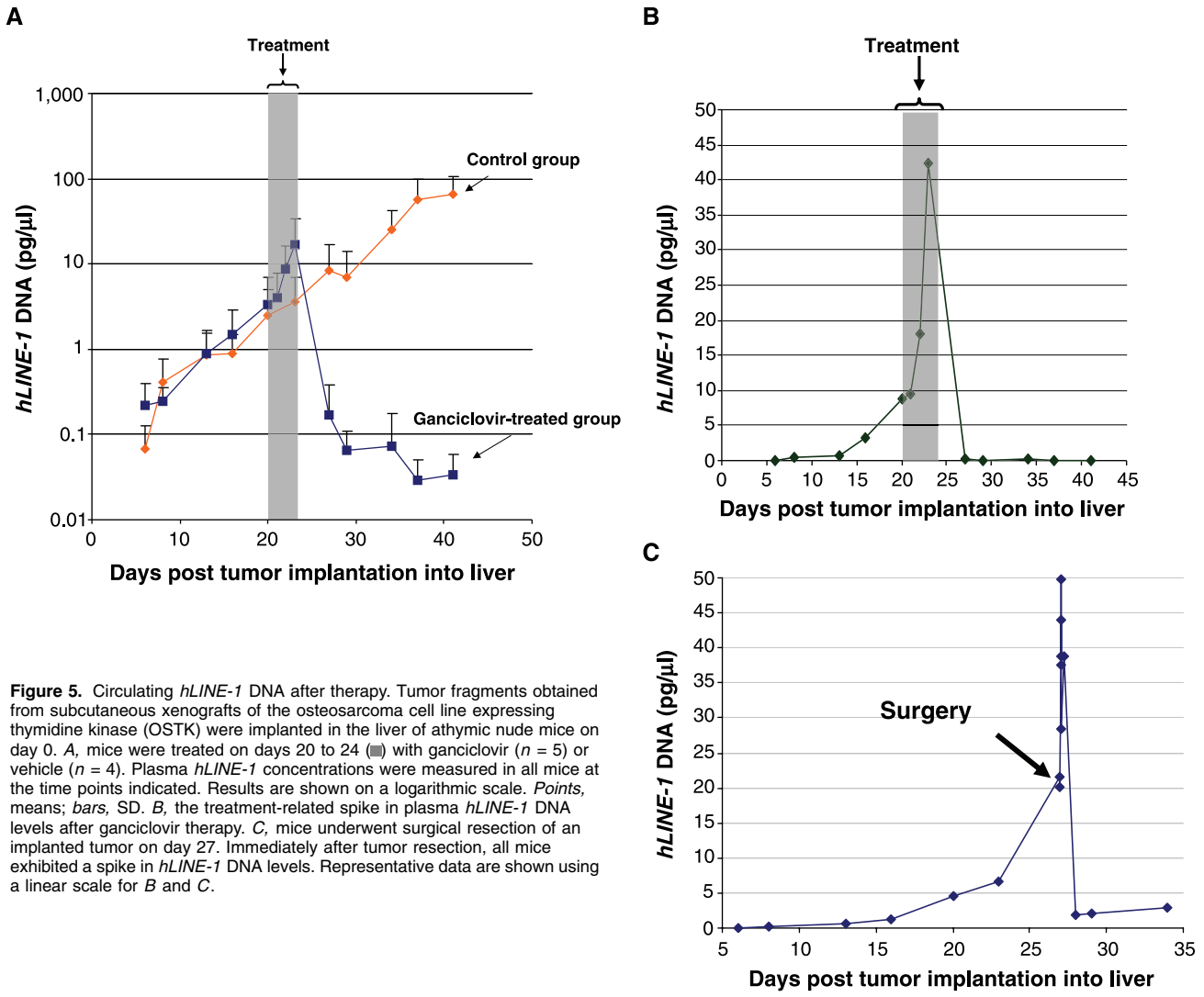

Figure 5. Circulating *hLINE-1* DNA after therapy. Tumor fragments obtained from subcutaneous xenografts of the osteosarcoma cell line expressing thymidine kinase (OSTK) were implanted in the liver of athymic nude mice on day 0. *A,* mice were treated on days 20 to 24 (▩) with ganciclovir (n = 5) or vehicle (n = 4). Plasma *hLINE-1* concentrations were measured in all mice at the time points indicated. Results are shown on a logarithmic scale. *Points,* means; *bars,* SD. *B,* the treatment-related spike in plasma *hLINE-1* DNA levels after ganciclovir therapy. *C,* mice underwent surgical resection of an implanted tumor on day 27. Immediately after tumor resection, all mice exhibited a spike in *hLINE-1* DNA levels. Representative data are shown using a linear scale for *B* and *C*.

made in this manuscript, if extendable to humans, also suggest that circulating tumor DNA may be a surrogate marker for tumor burden and can be used to rapidly predict the efficacy of cytotoxic anticancer agents. Recent reports from our group and others show that tumor-specific mutations can be detected and quantified in the circulation of patients with metastatic colorectal cancers and melanomas (27, 31). Future studies using circulating tumor-specific DNA from preclinical models and patients with cancer will further define the utility of these biomarkers in cancer research.

Acknowledgments

Received 2/13/2007; revised 6/14/2007; accepted 7/20/2007.

Grant support: The Virginia and D.K. Ludwig Fund for Cancer Research, The Miracle Foundation, The National Colorectal Cancer Research Alliance, and NIH grants CA43460, CA57345, and CA62924 (C. Rago, F. Diehl, V.E. Velculescu, K.W. Kinzler, B. Vogelstein, L.A. Diaz).

The costs of publication of this article were defrayed in part by the payment of page charges. This article must therefore be hereby marked *advertisement* in accordance with 18 U.S.C. Section 1734 solely to indicate this fact.

The authors thank Evangeline (Latice) Watson for excellent technical assistance, the staff of the Cancer Research Building animal facilities of the Sidney Kimmel Cancer Center for assistance with animal experiments, and Nickolas Papadopoulos and Eike Gallmeier for critical review.

References

1. Wiseman BS, Werb Z. Stromal effects on mammary gland development and breast cancer. Science 2002;296:1046–9.
2. Hu M, Yao J, Cai L, et al. Distinct epigenetic changes in the stromal cells of breast cancers. Nat Genet 2005;37:899–905.
3. Fidler IJ, Kim SJ, Langley RR. The role of the organ microenvironment in the biology and therapy of cancer metastasis. J Cell Biochem 2007;101:927–36.
4. Hart IR, Fidler IJ. Role of organ selectivity in the determination of metastatic patterns of B16 melanoma. Cancer Res 1980;40:2281–7.
5. Gupta GP, Massague J. Cancer metastasis: building a framework. Cell 2006;127:679–95.
6. Kerbel RS. Human tumor xenografts as predictive preclinical models for anticancer drug activity in humans: better than commonly perceived—but they can be improved. Cancer Biol Ther 2003;2:S134–9.
7. Garber K. Realistic rodents? Debate grows over new mouse models of cancer. J Natl Cancer Inst 2006;98:1176–8.
8. Weissleder R. Scaling down imaging: molecular mapping of cancer in mice. Nat Rev Cancer 2002;2:11–8.

9. Bouvet M, Tsuji K, Yang M, et al. *In vivo* color-coded imaging of the interaction of colon cancer cells and splenocytes in the formation of liver metastases. Cancer Res 2006;66:11293–7.

10. Liu HS, Jan MS, Chou CK, Chen PH, Ke NJ. Is green fluorescent protein toxic to the living cells? Biochem Biophys Res Commun 1999;260:712–7.

11. Shih IM, Torrance C, Sokoll LJ, et al. Assessing tumors in living animals through measurement of urinary β-human chorionic gonadotropin. Nat Med 2000;6:711–4.

12. Garcia-Olmo DC, Gutierrez-Gonzalez L, Ruiz-Piqueras R, Picazo MG, Garcia-Olmo D. Detection of circulating tumor cells and of tumor DNA in plasma during tumor progression in rats. Cancer Lett 2005;217:115–23.

13. Kim J, Yu W, Kovalski K, Ossowski L. Requirement for specific proteases in cancer cell intravasation as revealed by a novel semiquantitative PCR-based assay. Cell 1998;94:353–62.

14. Zijlstra A, Mellor R, Panzarella G, et al. A quantitative analysis of rate-limiting steps in the metastatic cascade using human-specific real-time polymerase chain reaction. Cancer Res 2002;62:7083–92.

15. Schneider T, Osl F, Friess T, Stockinger H, Scheuer WV. Quantification of human Alu sequences by real-time PCR—an improved method to measure therapeutic efficacy of anti-metastatic drugs in human xenotransplants. Clin Exp Metastasis 2002;19:571–82.

16. Kamat AA, Bischoff FZ, Dang D, et al. Circulating cell-free DNA: a novel biomarker for response to therapy in ovarian carcinoma. Cancer Biol Ther 2006;5:1369–74.

17. Samuels Y, Diaz LA, Jr., Schmidt-Kittler O, et al. Mutant PIK3CA promotes cell growth and invasion of human cancer cells. Cancer Cell 2005;7:561–73.

18. Sjoblom T, Jones S, Wood LD, et al. The consensus coding sequences of human breast and colorectal cancers. Science 2006;314:268–74.

19. Prak ET, Kazazian HH, Jr. Mobile elements and the human genome. Nat Rev Genet 2000;1:134–44.

20. Altschul SF, Gish W, Miller W, Myers EW, Lipman DJ. Basic local alignment search tool. J Mol Biol 1990;215:403–10.

21. Smit AF. Interspersed repeats and other mementos of transposable elements in mammalian genomes. Curr Opin Genet Dev 1999;9:657–63.

22. Kent WJ. BLAT—the BLAST-like alignment tool. Genome Res 2002;12:656–64.

23. Bauer TW, Parvizi J, Kobayashi N, et al. Diagnosis of periprosthetic infection: emerging antibiotic-resistant bacteria. Their treatment in total joint arthroplasty. J Bone Joint Surg Am 2006;88:869–82.

24. Urban C, Gruber F, Kundi M, et al. A systematic and quantitative analysis of PCR template contamination. J Forensic Sci 2000;45:1307–11.

25. Fleischhacker M, Schmidt B. Circulating nucleic acids (CNAs) and cancer—a survey. Biochim Biophys Acta 2007;1775:181–232.

26. Diehl F, Diaz LA, Jr. Digital quantification of mutant DNA in cancer patients. Curr Opin Oncol 2007;19:36–42.

27. Diehl F, Li M, Dressman D, et al. Detection and quantification of mutations in the plasma of patients with colorectal tumors. Proc Natl Acad Sci U S A 2005;102:16368–73.

28. Zirvi KA, Najjar TA, Slomiany BL. Sensitivity of human colon tumor metastases to anticancer drugs in athymic (nude) mice. Cancer Lett 1993;72:39–44.

29. Fournie GJ, Courtin JP, Laval F, et al. Plasma DNA as a marker of cancerous cell death. Investigations in patients suffering from lung cancer and in nude mice bearing human tumours. Cancer Lett 1995;91:221–7.

30. To EW, Chan KC, Leung SF, et al. Rapid clearance of plasma Epstein-Barr virus DNA after surgical treatment of nasopharyngeal carcinoma. Clin Cancer Res 2003;9:3254–9.

31. Shinozaki M, O'Day SJ, Kitago M, et al. Utility of circulating B-RAF DNA mutation in serum for monitoring melanoma patients receiving biochemotherapy. Clin Cancer Res 2007;13:2068–74.

Serial Assessment of Human Tumor Burdens in Mice by the Analysis of Circulating DNA

Carlo Rago, David L. Huso, Frank Diehl, et al.

Cancer Res 2007;67:9364-9370.